



Evaluating the impact of different exogenous factors on silk textiles deterioration with use of size exclusion chromatography

Dominika Pawcenis¹ · Mariusz Smoleń¹ · Monika A. Aksamit-Koperska¹ · Tomasz Łojewski^{1,2} · Joanna Łojewska¹

Received: 21 July 2015 / Accepted: 15 April 2016 / Published online: 9 May 2016
© The Author(s) 2016. This article is published with open access at Springerlink.com

Abstract Size exclusion chromatography (SEC), especially coupled with multiple angle laser light scattering detector (MALLS) is a powerful tool in diagnostics of deterioration of historic and art objects to evaluate their condition. In this paper, SEC–UV–MALLS–DRI technique was applied to study degradation of silk fibroin samples (*Bombyx mori*) artificially aged under various conditions: in the presence of oxygen, in different amount of water vapour and in volatile organic products (VOCs), all at temperature of 90 °C. Conditions were chosen in such a way that it mimicked real conditions of textiles' storing during exhibitions and in show cases. The influence of temperature, moisture and VOCs content on the state of silk textiles was examined with the use of size exclusion chromatography. Pseudo-zero-order Ekenstam equation was applied to study degradation rates of fibroin with use of the approximated values of DP of fibroin.

Abbreviations

DP	Degree of polymerisation
DRI	Differential refractive index detector
MALLS	Multiple angle laser light scattering detector
MWD	Molecular weight distribution

List of symbols

A_2	Second virial coefficient in Rayleigh equation
c	Concentration of a solution (mg/cm ³)
λ	Wavelength of incidental beam (in vacuum, nm)
k	Reaction's rate constant
K	Optical constant in Rayleigh's equation
M_n	Number average molar mass (g/mol)
M_w	Weight average molar mass, derived from Rayleigh equation (g/mol)
n_0	Refractive index of a solvent
N_A	Avogadro constant
dn/dc	Refractive index increment
$P(\theta)$	Form factor in Rayleigh equation
$R(\theta)$	Excess Rayleigh ratio, the difference between Rayleigh ratio for a solution and a pure solvent

1 Introduction

Silk fibres have been used since 3500 B.C. in the textile industry, thanks to their unique properties like strength, moisture absorption and lustre. For this reason, many objects of historic importance are made of silk fibres. Thus, many museums have silk garments, carpets, tapestries and banners in their collections [1]. Exhibition of textiles allows the wide audience to enjoy history, beauty and craftsmanship of these silks. Regrettably, silk included in historical objects undergoes natural degradation induced by light, temperature, humidity and other factors; it turns yellow and loses the mechanical strength [1]. Since in today's societies there is a high demand for preservation of the historical objects of cultural heritage importance, the question arises how to preserve and conserve them for future generations. Active conservation treatments can alter their appearance which will affect their artistic

✉ Joanna Łojewska
lojewska@chemia.uj.edu.pl

¹ Chemistry Faculty, Jagiellonian University, Ingardena 3, 30-060 Kraków, Poland

² Faculty of Materials Science and Ceramics, AGH University of Science and Technology, Mickiewicza 30, B8/3.36, 30-059 Kraków, Poland

performance. Alternatively, passive conservation methods are applied to extend the lifetime of silk objects by developing methods for their safe exposition, preservation and storage.

Characteristic properties of silk result from the molecular architecture of fibroin, of which silk fibre is mostly consisted. The primary structure is created by a sequence of amino acids, mainly by glycine (45 %), alanine (29 %), serine (12 %) and tyrosine (5 %). Leucine, proline, valine, phenylalanine, histidine, lysine, threonine, arginine are the less abundant amino acids in fibroin [1–3]. The secondary structure is determined by the particular amino acids, which create rigid crystalline regions, arranged in the structure of β -harmonica, located in the heavy chain. This secondary structure is a result of the dominance of the hydrophobic amino acids such as glycine and alanine, arranged in parts of 59-mer-a repeating sequence of GAGAGSGAAG[SGAGAG]₈Y [4, 5]. Ordered crystalline regions making up about 60 % of the fibroin mass [6] are interspersed with amorphous regions located in the area of the light chain [7]. These regions are richer in the hydrophilic amino acids such as serine, threonine, arginine and lysine, which are more susceptible to degradation [8–12].

Different storage and exhibition conditions have seriously affected the current condition of silk objects. Light, temperature and humidity have a detrimental impact on the rate of the degradation, manifested by, for example, glass transition [13], recrystallisation [14, 15], oxidative [16–19] and photooxidative [20, 21] changes, and photoinduced –S–S– bond breakdown [22, 23]. Additionally, the material during natural ageing emits volatile organic compounds (VOCs), which results in mass loss [24]. VOCs like acetic acid may also contribute to acidic hydrolysis [24]. The oxidation reactions were examined broadly by Shao et al. [25], who presented results of investigations on changes in the crystallinity of fibroin as a function of the compactness of tyrosine, studied through ATR-FTIR and FT-Raman spectroscopies. Artificial ageing of silk fibres induced by the factors mentioned above is hoped to mimic the natural processes to better understand the degradation phenomena.

What is known about thermal ageing of silk, used in this study, is that its effects can be classified into two groups: purely physical (structural) changes within a fibroin fibre, and chemical changes. High temperature induces the changes in its amino acids composition of fibroin [16, 19, 26] and to the scissions of its chains, which in turn results in the changes in molar mass distribution. It also enhances the formation of oxygen free radicals [27, 28], which attack the most reactive amino acids: tryptophan, tyrosine and phenylalanine in amorphous regions [23, 29]. This eventually gives rise to the loss of silk brightness [19, 24, 30]. Oxidative changes in functional groups of fibroin chains lead to their spatial rearrangement within amorphous

regions [14, 18], which together with water vapour, VOCs, oxygen or other agents facilitate chain scission. Additionally, upon thermal treatment a decrease in basic amino acids content and increase of the amount of acidic amino acids is observed [31].

By determining degradation mechanism and then kinetic parameters that rule the observed degradation changes, many important questions concerning the collection preservation could be answered. One of them is the identification of silk object and their dating, and another is risk assessment. The knowledge of the degradation mechanism in principle allows to inhibit degradation pathways by designing the storage atmosphere so that it prevents their occurrence or by the chemical treatment of the textiles. A simple way of altering the storage conditions is for example lowering the temperature. According to Michalski et al. [32], a 5 °C decrease in temperature will significantly prolong the lifetime of temperature-sensitive materials, analogously to the estimation that chemical reaction rates are reduced by a half for each 10 °C fall. The interaction with relative humidity (RH) for other natural polymer–cellulosic materials was also described [32, 33], and it was demonstrated that a power law fits the data best.

Accordingly to the expected changes in the silk fibres' structure and composition, different analytical methods can be applied. In the literature, the degradation was evaluated by the changes of silk mechanical properties [34], colour [30], crystalline structure by X-ray diffraction [14, 18, 35], viscosity [36, 37], molecular weight of silk component by sodium dodecyl sulphate-polyacrylamide gel electrophoresis (SDS-PAGE) [38] and molecular weight distribution by SEC [19, 30, 36, 39–41]. As the macroscopic properties (like mechanical endurance) of silk textiles may be reflected by the distribution of fibroin chain length, condition of the historical silk textiles can be evaluated from measurements of the molecular weight distribution of the silk [ref]. Thus, silk samples are quite commonly analysed by size exclusion chromatography (SEC) coupled with different detectors: ultraviolet spectrophotometric (UV), MALLS and differential refractive index (DRI) detectors.

Indeed, molecular weights (which sometimes can be expressed as the degree of polymerisation) of aged cellulosic and silk materials can be used in the study of degradation kinetics. Whereas kinetics of cellulose degradation has been widely studied [33, 42–48], there is still a gap in knowledge about silk fibroin's kinetics of degradation [40, 49, 50]. Literature data are limited to kinetics and activation energies derived from tensile testing [40, 51] and thermal analysis [52]. However, the latter one may not reflect silk degradation occurring on open display at room temperature, which creates the necessity of investigation of the influence of temperature and RH on silk textiles deterioration.

Assuming that depolymerisation is a pseudo-zero-order reaction, a kinetics of degradation of linear polymers can be described by Ekenstam equation:

$$\ln\left(1 - \frac{1}{DP_0}\right) - \ln\left(1 - \frac{1}{DP_t}\right) = kt \quad (1)$$

where k is a reaction rate constant, t is time of ageing, DP_t and DP_0 are degrees of polymerisation of aged and unaged polymer, respectively. According to Luxford, number average molecular weight might be used instead of DP in case of silk fibroin [40]; however, in the same work Luxford reports on the basis of HPSEC and tensile strength results that M_n may be not equivalent to DP, like in cellulose. As a matter of fact, in the case of polypeptides it is almost impossible to accurately compute DP due to different molar masses of amino acids building up a polypeptide chain. Unlike DP, molar mass of any polymer will not directly reflect the number of chemical bonds between mers in polymer chain which could be used to define the degradation rate. For this reason, it seems that the use of any average molar mass in kinetic studies of silk fibroin is inadequate.

In this work, special attention is paid to the silk degradation via depolymerisation process, facilitated by a number of factors that occur naturally in the museums' environment. To spot possible degradation pathways, a thermal ageing in 90 °C in oxygen atmosphere was applied, coupled with different humidity levels and in presence of VOCs. These factors are known to affect art materials at a different rate [18, 30, 33, 40, 49, 51, 53–55]. The deterioration of silk fibres causes brittleness of the textile, resulting in loss of mechanical endurance. It is known that elevated relative humidity favours hydrolytic [18, 40] and microbial [56–59] and oxidative [18] degradation of silk textiles. On other hand, accelerated ageing experiments on silk textiles indicated that dry-air atmosphere causes effects similar to damages detected in historic samples [19, 60].

To evaluate the influence of relative humidity, presence of oxygen and volatile products of material degradation on silk textiles, it seems reasonable to compare material aged at the same elevated temperature at different RH, and in open and closed reactors (the latter to study the impact of

degradation products in the ageing atmosphere). An attempt to determine kinetic parameter in first-order kinetics approximation (k) values has been undertaken based on the results of molecular masses determined by SEC of the samples aged at different conditions.

2 Experimental

2.1 Samples of silk fibroin and artificial ageing

Standard degummed and bleached silk fabric from *Bombyx mori* (Habotai 35 g/m² Fei-Long, Warsaw, Poland) was used in all experiments.

Prior to accelerated ageing, the samples were cut into pieces (c.a. 0.07 g) and dried for 15 min at 110 °C in order to desorb water, and so not to distort the calculated relative humidity with in the ageing chamber and vials.

The accelerated ageing experiments were performed in three types of reactors providing number of conditions, presented in Table 1.

During artificial ageing tests, samples were hanged in the thermal ageing chamber (open reactor) or in closed vials and heated up to 90 °C. By changing the reactor type and gaseous conditions, the influence of several environments could be traced down. Artificial ageing lasted 1, 3, 5, 7, 14, 21, 28 and 35 days, allowing monitoring long time changes. Samples aged in closed vessels in 0 and 30 % RH were aged only for 14 days.

Moisture content in ageing vessels was adjusted to obtain variety of conditions: from dry, semi-humid to humid, with RH values equal, correspondingly, to 0, 30 and 70 % RH as calculated for 293 K and 1013 hPa.

Volatile organic compounds' influence on silk degradation was imitated by ageing in hybridisation vials, acting as closed air-tight reactors [61]. Samples of c.a. 0.07 g of textile were put in c.a. 150 cm³ volume hybridisation glass vials and were tight locked. The amount of silk was calculated so that the amount of oxygen in the vials was sufficient to assure a total oxidation of all N, C and S atoms in the fibroin molecule. Detailed description of ageing conditions and their supposed influence is depicted in Table 1.

Table 1 Ageing conditions and agents affecting aged material

Reactor	Type	Conditions	Impact
Dryer	Open (air circulation)	Oxygen $T = 90\text{ °C}$	T + O ₂
Climatic chamber	Open	Oxygen 70 % RH $T = 90\text{ °C}$	T + O ₂ + H ₂ O
Closed vial	Closed	Oxygen	T + O ₂ + H ₂ O + VOC

2.2 Size exclusion chromatography

2.2.1 Sample preparation

Sample preparation procedure was described in details in previous work [39]. In the current work, dissolution of silk samples in 9.3 M LiBr (at 60 °C for 3 h) was followed by dialysis in a cellulose membrane tube (molecular weight cut-off 3.5 kDa, ZelluTrans/Roth T1) against pure water (specific resistivity 18.2 MΩ, Simplicity 185 Merck Millipore) for 4 h in microdialysis capsules a'1 cm³ QuixSep (Roth). The dialysis solution was exchanged every 30 min in order to remove LiBr. The final solutions for SEC analysis were prepared by mixing one volume of 0.4 M NaCl solution with one volume of each sample in order to obtain silk fibroin in 0.2 M NaCl. Prior to SEC analyses, samples were centrifuged.

Transparent silk fibroin solutions without visible suspended particles were subjected to further analysis without filtration.

2.2.2 Analyses

The SEC system consisted of the following items: Waters 1515 isocratic pump, Waters 717+ auto sampler, a column oven, a UV–Vis detector (Waters 2487 Dual λ Absorbance, set at the wavelength 280 nm), a multiple angle laser light scattering detector Dawn Heleos (Wyatt Technology) and a differential refractive index detector Optilab T-rEX (Wyatt Technology), acting as a concentration-sensitive detector. Both MALLS and RI worked at the same wavelength (658 nm). In the literature, such SEC configuration for protein analyses is well described [62].

Chromatographic separation was performed on silica-based column Yarra SEC S-4000 from Phenomenex (packed 3 μm, 300 × 7.8 mm), maintained at 30 °C (the same temperature as in DRI detector), a downstream guard column was used (Phenomenex, 300 × 4.6 mm). 0.2 M NaCl (aqueous solution, water from Simplicity 185 system, Merck Millipore) was used as a mobile phase, with a flow rate of 0.30 cm³/min. Silk fibroin samples were injected in volumes ranging from 30 to 75 μl. Each sample was analysed 3 times. The specific refractive index increment of fibroin was determined in batch mode using differential refractive index detector Optilab T-rEX and calculated in Astra 6.0.2 software (Wyatt Technology).

3 Data processing/calculations

3.1 Chromatographic results

The determination of absolute values of molecular weights using size exclusion chromatography with MALLS detection is based on Rayleigh equation:

$$\frac{K \times c}{R_\theta} = \frac{1}{M_w P(\theta)} + 2A_2 c \quad (2)$$

where K is a combined constant including the refractive index increment dn/dc :

$$K = \left(2\pi^2 n_0^2 \left(\frac{dn}{dc} \right)^2 \right) \left(\frac{1 + \cos^2 \alpha}{N_A \lambda_0^4} \right) \quad (3)$$

In order to apply Rayleigh equation, number of parameters must be known: fibroin concentration c , its specific refractive index increment dn/dc and second virial coefficient A_2 . A_2 is usually neglected due to small concentrations applied.

Concentration values came from differential refractive index detector (concentration sensitive). Specific refractive index value was obtained from three batch measurements of five different concentration of fibroin in water, ranging from 0.01 to 1.0 mg/cm³ and was equal to 0.1999 ± 0.007 cm³/g.

Weight average molar mass from Rayleigh equation was calculated with the use of Debye's model, which is recommended for large molecules [63, 64]. A plot of $R_\theta/K \times c$ versus $\sin^2(\theta/2)$ was constructed. The plot was fitted by a linear regression to obtain the intercept at zero angle as well as the slope at zero angle.

Calibration of MALLS detector requires determination of detector constant which is a proportionality factor between the detector signal and the Rayleigh coefficient $R(\theta)$ for one photodiode (11th, on 90°). The detector constant determination was performed with toluene (HPLC purity) and was found to be 1.5151×10^{-4} 1/V × cm. Further procedure includes normalisation of other 17 photodiodes, which was done using a bovine serum albumin (BSA) standard (66 kDa, Roth). Interdetector delay for UV–MALLS and MALLS–DRI was determined with the value of 0.0157 and 0.8709 cm³, respectively, also with the use of BSA.

3.2 Kinetics of degradation

To obtain k value from kinetic curves, a reciprocal of M_n or M_w versus ageing time may be plotted. However, as we mentioned in Sect. 1, M_n and M_w may not be suitable to reflect the total number of peptide bonds. For this reason, we decided to use approximate degree of polymerisation of fibroin. Basing on the percentage and molar masses of particular amino acids in fibroin, a weighted average molar mass of a “monomer” was calculated and was equal to 93.46 g/mol, designated further as M_m (Eq. 4). Details regarding calculations of M_m are presented in Table 2.

$$M_m = \frac{\sum m_i w_i}{\sum w_i} \quad (4)$$

Table 2 Abundance of amino acids in fibroin and calculation of weight averaged molar mass of a “monomer” amino acid

Amino acid	Molar mass, g/mol (m_i)	Contribution (w_i)	$m_i \times w_i$, g/mol
G	75.07	0.45	33.78
A	89.09	0.29	25.84
S	105.09	0.12	12.61
Y	181.19	0.05	9.06
V	117.15	0.02	2.34
D	133.1	0.01	1.33
R	156.19	0.01	1.56
E	147.13	0.01	1.47
I	131.17	0.01	1.31
L	131.17	0.01	1.31
F	165.19	0.01	1.65
T	119.12	0.01	1.19
		$\Sigma w_i = 1.00$	$\Sigma m_i \times w_i$
		$M_m = 93.46$ g/mol	$= 93.46$ g/mol

By dividing a weight average molar mass (Eq. 5) of fibroin samples obtained from SEC–MALLS, we obtained approximated DP value (Eq. 6).

Weight average molar mass was calculated from equation:

$$M_w = \frac{\sum N_i M_i^2}{\sum N_i M_i} \quad (5)$$

$$DP = \frac{M_w}{M_m} \quad (6)$$

Details regarding calculations of M_m are presented in Table 2.

Reciprocal of DP values for each condition sets (dry air ageing, wet air ageing in climatic chamber and ageing in closed vials) against ageing time were fitted to obtain linear dependence, expressed in Eq. 1. From slopes of kinetic curves k values were derived.

It has to be emphasized that the approach presented here is a kind of generalisation, which is based on two simplifications:

1. Polymer chain scission runs with the same rate in the crystalline and amorphous regions;
2. Amino acid composition is the same in the crystalline and amorphous region.

Regarding the first assumption, it is known that amorphous regions are easily degraded due to better accessibility of degradation agents such as VOCs, water vapour, oxygen [9–11, 50], unlike tightly packed crystalline regions. The second assumption has its consequences in the calculation of DP. The method of calculation proposed here bases on the

average percentage of particular amino acids in silk fibroin chains, though amino acid composition in amorphous regions differs from crystalline ones. This also results in the generalisation used in our the kinetics approach, as in the silk protein the most abundant amino acids are glycine and alanine, which are relatively light molecules and built mostly of crystalline phase [4, 65, 66]. Taking into account that silk fibroin is constructed of about 60–70 % of crystalline regions [66], the first assumption gives overestimation of rate constant value, k , while the second simplification exerts an opposite effect on the k value.

In fact, in order to create a real picture of the kinetics of silk fibroin degradation, the reactions running in the amorphous and crystalline regions should be considered separately, due to different mass transport rates and susceptibility of amino acids to the degradation agents in these two domains. However, in real samples of silk fibroin used in this study it was impossible to isolate crystalline regions from amorphous ones, thus we could only make approximations to describe the rate of depolymerisation process in fibroin chains.

4 Results

4.1 Molecular weight distribution of silk fibroin

Molecular weight distribution (MWD) curves of aged samples compared with unaged one (Figs. 1, 2) distinctly shift towards lower values of molar mass regardless of the ageing conditions used, and initially they have rather monomodal distribution. However, after longer ageing time a shoulder peak appears indicating the appearance of a new fibroin fraction of a lower molecular weight, especially for the samples aged at elevated humidity in a climatic chamber and in closed vials. In Fig. 1a–c, the results are arranged in a sequence of growing number of degradation agents: from O₂ through O₂ and H₂O (70 % RH) to finally O₂, H₂O (70 % RH) and VOC. For samples aged in dry air, the changes in MWD are the least, the range of MMD curves is between 31.5 and 1000 kDa. It is not surprising that oxidation is a dominating reaction during ageing in dry air which has been observed in the literature for both silk and cellulose [18, 53, 67, 68], which explains why depolymerisation of the polypeptide is not a prevailing reaction here. This oxidation can, however, bring about the chain breakage and in this way contribute to the drop in its molecular weight. The addition of water vapour to the degradation atmosphere causes more significant changes in distribution of fibroin chains length (Fig. 1b), manifested by more significant decrease of molecular mass (from 3.15 to 1000 kDa) especially in the final period of ageing (last 7 days). It is interesting to note that VOC, another gas

phase agents that appears during ageing in a closed reactor, gives rise to slightly lesser degradation effect than the water vapour alone although the degradation dynamics is higher at the initial stage of ageing.

The influence of VOC on the degradation progress is presented in Fig. 2a–c. In this experimental series, the shorter ageing was applied than in the previous series and the experiments differ in the growing concentration of water vapour starting from 0 through 125 g/m³ (30 % RH) to 293 g/m³ (70 % RH). The greatest drop in molecular mass is observed for the samples aged at relative humidity of 70 %, where overall deterioration is powered by high water concentration. In fact, acidic VOCs like acetic acid clearly contribute to acid hydrolysis of polypeptide chain

[24]. However, regardless of the level of relative humidity, the final degradation stage of fibroin seems to be similar which may indicate that during ageing the recrystallisation also takes place which inhibits further degradation [18, 19]. The negative influence of moisture on silk fibres was noted in the literature [18, 39, 40]. Depending on the humidity level, the degradation dynamic is different, in VOC the most significant changes appear in the final ageing stage, while with increasing water vapour concentration degradation accelerates in the beginning of degradation. It seems the role of water in degradation mechanism is at least twofold where it acts as hydrolysis substrate on the one hand and as a polymer plasticizer facilitating the polypeptide access to degradation agents, on the other.

Fig. 1 Molecular weight distribution shifts of silk fibroin samples aged in: **a** ventilated oven, **b** climatic chamber with controlled RH level at 70 %, **c** sealed vial containing water vapour corresponding to 70 % RH

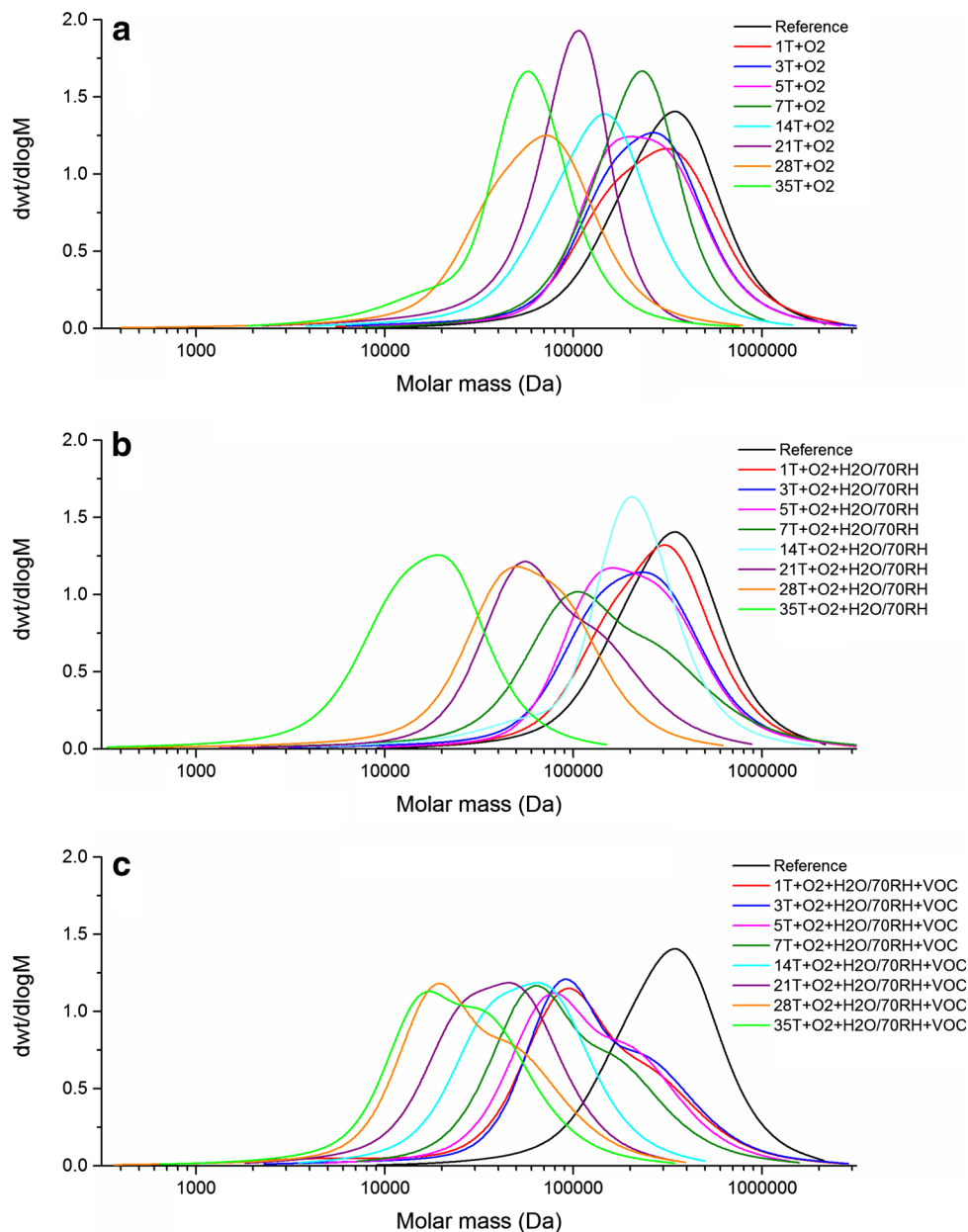
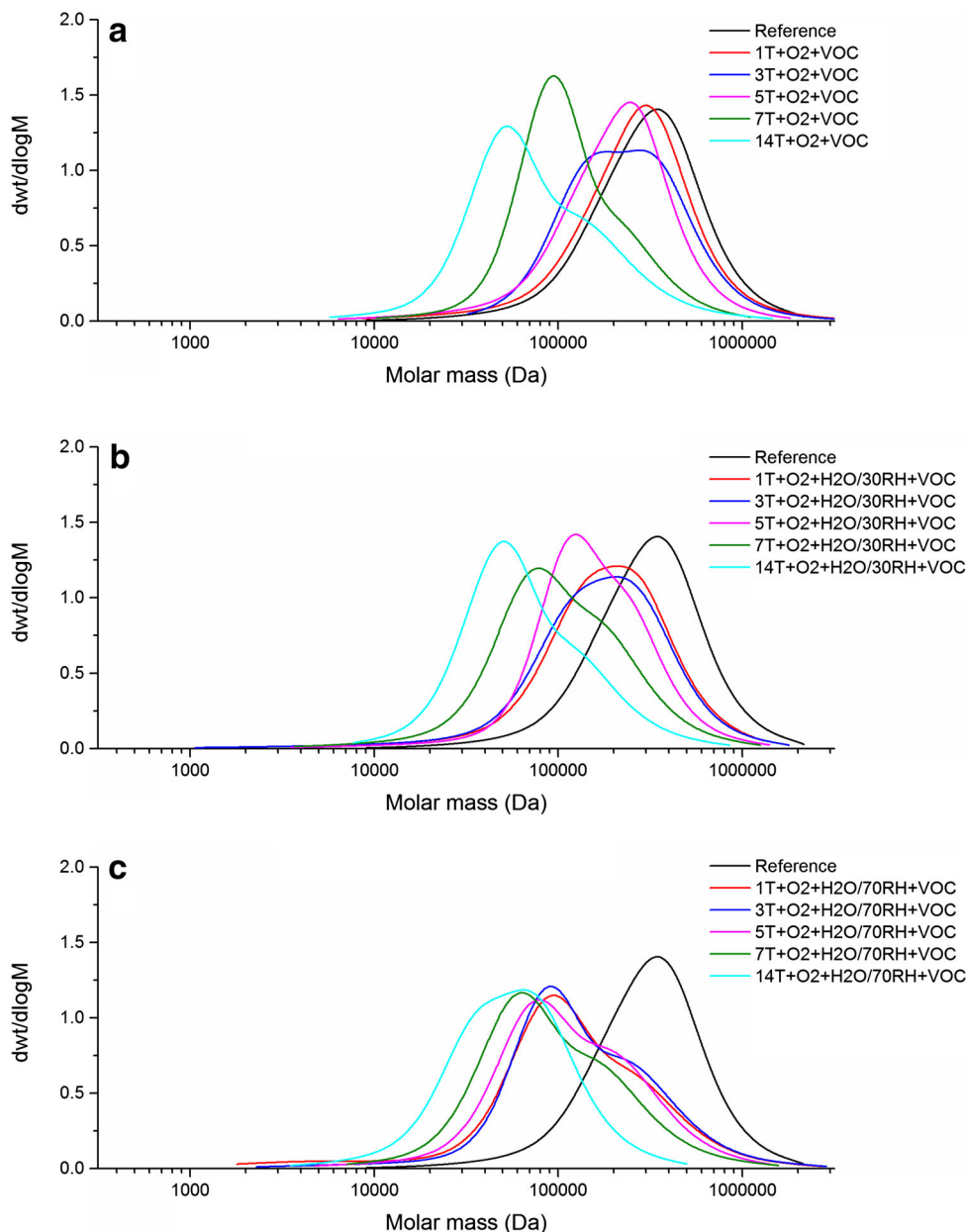


Fig. 2 Molecular weight distribution curves of silk fibroin samples aged in sealed vials at different relative humidity levels: **a** 0 % RH, **b** 30 % RH, **c** 70 % RH



Additionally, water may act as a transport media for both protons in acidic hydrolysis (H_3O^+) and radicals in oxidation (e.g. OH^*). The polymodal distribution of molar masses of aged samples may suggest that there are more and less stable fractions of fibroin that undergo degradation with higher and lower rates. These two fractions can be combined with the presence of amorphous and crystalline phases of fibroin which indeed degrade with different rates.

4.2 Ageing conditions vs degradation progress

To evaluate the impact of relative humidity and presence of VOCs on degradation more quantitatively, the degradation progress was expressed as DP dependence on ageing time.

Assuming the pseudo-zero-order approximation of first-order kinetic equation (Eq. 1), rate constant values, k , can be derived from Eq. 7:

$$kt = \frac{1}{\text{DP}_t} - \frac{1}{\text{DP}_0} \quad (7)$$

According to Eq. 7, $1/\text{DP}_0 - 1/\text{DP}_t$ is a measure of the number of broken bonds [69, 70]. In cellulose for low values of DP, a downward or upward curvature of the $1/\text{DP}$ vs time was observed [71–73], which may suggest that kinetic equation is applicable only at early stages of depolymerisation. From the Fig. 3, it can be deduced that for silk fibroin similar situation takes place. The k values are consistent within two groups of conditions: without

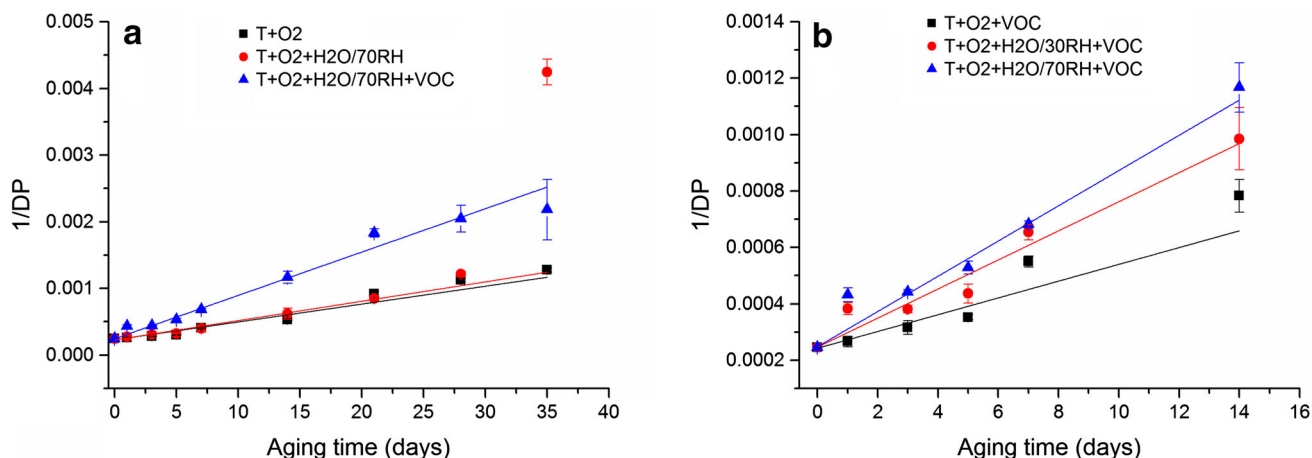


Fig. 3 Relation between reciprocal of DP versus ageing time: **a** ventilated oven, climatic chamber with controlled RH level at 70 %, and sealed vial containing water vapour corresponding to 70 % RH, **b** sealed vials with 0, 30, 70 % RH

Table 3 k values derived from DP of samples aged at dry and elevated humidity levels and VOCs atmosphere

Ageing conditions	k (day ⁻¹)	Error	R^2
T + O ₂	2.7E-5	2.7E-6	0.923
T + O ₂ + H ₂ O/70RH	2.9E-5	5.9E-6	0.746
T + O ₂ + H ₂ O/70RH + VOC	6.5E-5	3.4E-6	0.978
T + O ₂ + VOC	3.0E-5 ^a	5.5E-6	0.848
T + O ₂ + H ₂ O/30RH + VOC	5.2E-5 ^a	6.6E-6	0.923
T + O ₂ + H ₂ O/70RH + VOC	6.3E-5 ^a	4.1E-6	0.980

^a Ageing interval limited to 14 days

water vapour independently of conditions applied k drops to the range from 2.7×10^{-5} to 3.0×10^{-5} 1/day. Water vapour seems to considerably enhance degradation progress and change degradation mechanism which is reflected by much higher k values falling into the range from 5.2×10^{-5} to 6.5×10^{-5} 1/day (Table 3). Thus, notwithstanding the physical meaning of k , it can be used as a gauge to assess degradation progress. The trend in k is consistent with the literature data concerning recommendations for textiles storage.

An influence of water vapour on the degradation mechanism can only be speculated here. Water indubitably accelerates the hydrolysis being a necessary substrate for its occurrence [74]. In such a case, kinetic equation should comprise water vapour concentration in another approach to the degradation kinetics. Secondly, water is a known polypeptide plasticizer [75–78] which rearranges hydrogen bond network [79, 80] providing new diffusional paths for both hydrolysis and oxidation reactions. When radical mechanism of oxidation is assumed which can also be accompanied by the peptide bond scission, water can play a role of a transporter or provider of radicals.

5 Conclusions

The aim of this work was to approximate the kinetics of fibroin degradation at various conditions. The influence of temperature, moisture and VOCs content on the state of silk textiles was surveyed with the use of size exclusion chromatography. Based on the results of molecular mass, distributions of the approximated values of DP were calculated. They served as kinetic variables to study degradation rates of fibroin approximated by pseudo-zero-order Ekenstam equation. Destructive influence of water vapour on silk fibres was confirmed by the values of rate constants which validates the kinetic equation applied.

Acknowledgments Financial support from the National Science Centre (Decision No. 2014/13/N/ST4/04089) and European Union (“Doctus” scholarship to D.P.) is kindly acknowledged. The size exclusion chromatography system was equipped with a differential refractive index detector, which was purchased thanks to the financial support of the European Regional Development Fund in the framework of the Polish Innovation Economy Operational Programme (Contract No. POIG.02.01.00-12-023/08).

Open Access This article is distributed under the terms of the Creative Commons Attribution 4.0 International License (<http://creativecommons.org/licenses/by/4.0/>), which permits unrestricted use, distribution, and reproduction in any medium, provided you give appropriate credit to the original author(s) and the source, provide a link to the Creative Commons license, and indicate if changes were made.

References

1. A. Timar-Balazsy, D. Eastop (eds.), *Chemical Principles of Textile Conservation* (Butterworth-Heinemann, Oxford, 1988)
2. S. Landi (ed.), *Textile Conservator's Manual*, 2nd edn. (Butterworth-Heinemann, Oxford, 1998)

3. R.B.D. Fraser, T.P. MacRae, in *Conformation of Fibrous Proteins and Related Synthetic Polypeptides* (Academic Press, New York, 1973), pp. 293–343
4. C.Z. Zhou, F. Confalonieri, M. Jacquet, R. Perasso, Z.G. Li, J. Janin, *Proteins* **44**, 119 (2001)
5. D. Kaplan, W.W. Adams, B. Farmer, C. Viney, in *Silk: Biology, Structure, Properties, and Genetics*, ed. by D. Kaplan, W.W. Adams, B. Farmer, C. Viney (American Chemical Society, Washington, 1994), pp. 2–16
6. K. Urich, *Comparative Animal Biochemistry* (Springer, New York, 1994), pp. 394–397
7. M. Lewin, *Handbook of Fiber Chemistry*, 2nd edn. (CRC Press, Boca Raton, 2006)
8. Y. Hu, Q. Zhang, R. You, L. Wang, M. Li, *Adv. Mater. Sci. Eng.* **2012**, 185905 (2012). doi:10.1155/2012/185905
9. Y. Cao, B. Wang, *Int. J. Mol. Sci.* **10**, 1514 (2009)
10. C. Vepari, D.L. Kaplan, *Prog. Polym. Sci.* **32**, 991 (2007)
11. S. Inoue, K. Tanaka, F. Arisaka, S. Kimura, K. Ohtomo, Sh. Mizuno, *J. Biol. Chem.* **275**(51), 40517–40528 (2000)
12. Y. Yanagi, Y. Kondo, K. Hirabayashi, *Text. Res. J.* **70**, 871 (2000)
13. N. Agarwal, D.A. Hoagland, R.J. Farris, *J. Appl. Polym. Sci.* **63**, 401 (1996)
14. P. Garside, P. Wyeth, *Appl. Phys. A* **89**, 871 (2007)
15. P. Garside, S. Lahlil, P. Wyeth, *Appl. Spectrosc.* **59**, 1242 (2005)
16. I. Vanden Berghe, *J. Archaeol. Sci.* **39**, 1349 (2012)
17. M. Koperska, T. Łojewski, J. Łojewska, *Spectrochim. Acta. A. Mol. Biomol. Spectrosc.* **135**, 576 (2015)
18. M.A. Koperska, D. Pawcenis, J. Bagniuik, M.M. Zaitz, M. Missori, T. Łojewski, J. Łojewska, *Polym. Degrad. Stab.* **105**, 185 (2014)
19. F. Vilaplana, J. Nilsson, D.V.P. Sommer, S. Karlsson, *Anal. Bioanal. Chem.* **407**, 1433 (2015)
20. C. Solazzo, J.M. Dyer, S. Deb-Choudhury, S. Clerens, P. Wyeth, *Photochem. Photobiol.* **88**, 1217 (2012)
21. Z. Wang, W. Chen, Z. Cui, K. He, W. Yu, *J. Text. Inst.* **107**(4), 413–419 (2015). doi:10.1080/00405000.2015.1034933
22. A. Sionkowska, A. Planecka, *Polym. Degrad. Stab.* **96**, 523 (2011)
23. S. Baltova, V. Vassileva, *Polym. Degrad. Stab.* **60**, 53 (1998)
24. M.A. Koperska, D. Pawcenis, J.M. Milczarek, A. Blachecki, T. Łojewski, J. Łojewska, *Polym. Degrad. Stab.* **120**, 357 (2015)
25. J. Shao, J. Zheng, J. Liu, C.M. Carr, *J. Appl. Polym. Sci.* **96**, 1999 (2005)
26. I. Vanden Berghe, J. Wouters, in *Identification and Condition Evaluation of Deteriorated Protein Fibres at the Sub-Microgram Level by Calibrated Amino Acid Analysis*, ed. by R. Janaway, P. Wyeth (Archetype Publications, London, 2005), pp. 151–158
27. P. Garside, P. Wyeth, in *Conservation Science: Heritage Materials*, ed. by E. May, M. Jones (Royal Society of Chemistry, Cambridge, 2006), pp. 56–91
28. D. Gong, H. Yang, *Polym. Degrad. Stab.* **98**, 1780 (2013)
29. X. Zhang, I. Vanden Berghe, P. Wyeth, *J. Cult. Herit.* **12**, 408 (2011)
30. J. Kim, P. Wyeth, *E-Preservation* **6**, 60 (2009)
31. H.E. Ahmed, S.S. Darwish, *J. Polym. Environ.* **20**, 596 (2012)
32. S. Michalski, in *ICOM Comm. Conserv. 10th Trienn. Meet. Washington, DC, 22–27 August 1993 Prepr.* (1993), pp. 624–629
33. D. Erhardt, M. F. Mecklenburg, in *Mat. Res. Soc. Symp. Proc.* (1995), pp. 247–270
34. P. Wyeth, in *Signatures of Ageing: Correlations with Behaviour*, ed. by R. Janaway, P. Wyeth (Archetype Publications, London, 2005), pp. 137–142
35. A.C. Hermes, R.J. Davies, S. Greiff, H. Kutzke, S. Lahlil, P. Wyeth, C. Rieke, *Biomacromolecules* **7**, 777 (2006)
36. S. Tse, A. Dupont, in *Hist. Text. Pap. Polym. Museums*, edited by J. M. Cardamone and M. T. Baker (ACS Symposium Series, American Chemical Society, Washington, DC, 2001), pp. 98–114
37. X. Zhang, S. Yuan, *Chin. J. Chem.* **28**, 656 (2010)
38. H. Yamada, H. Nakao, Y. Takasu, K. Tsubouchi, *Mater. Sci. Eng. C* **14**, 41 (2001)
39. D. Pawcenis, M.A. Koperska, J.M. Milczarek, T. Łojewski, J. Łojewska, *Appl. Phys. A* **114**, 301 (2013)
40. N. Luxford, *Reducing the Risk of Open Display: Optimising the Preventive Conservation of Historic Silks*, Doctoral Thesis, University of Southampton, Winchester School of Art (2009)
41. K. Hallet, D. Howell, in *Size Exclusion Chromatography as a Tool for Monitoring Silk Degradation in Historic Tapestries*, ed. by R. Janaway, P. Wyeth (Archetype Publications, London, 2005), pp. 143–150
42. P. Calvini, *Cellulose* **21**, 1127 (2014)
43. A.M. Emsley, G.C. Stevens, *Cellulose* **1**, 26 (1994)
44. A. Emsley, R. Heywood, M. Ali, C. Eley, *Cellulose* **4**, 1 (1997)
45. M. Kes, B.E. Christensen, *Cellulose* **20**, 2003 (2013)
46. *Step Project CT 90-0100, The Effects of Air Pollutants on the Accelerated Ageing of Cellulose Containing Materials—Paper* (Delft, 1994)
47. A. Quye, D. Littlejohn, R.A. Pethrick, R.A. Stewart, *Polym. Degrad. Stab.* **96**, 1934 (2011)
48. H.Z. Ding, Z.D. Wang, *Cellulose* **14**, 171 (2007)
49. N. Luxford, D. Thickett, *J. Inst. Conserv.* **34**, 115 (2011)
50. Q. Lu, B. Zhang, M. Li, B. Zuo, D.L. Kaplan, Y. Huang, H. Zhu, *Biomacromolecules* **12**, 1080 (2011)
51. N. Luxford, D. Thickett, P. Wyeth, in *Preserving Silk: Reassessing Deterioration Factors for Historic Silk Artefacts*, ed. by C.A. Wilson, R.M. Laing (The Textile Institute (NZ), Dunedin, 2009), pp. 151–157
52. M.N. Bora, G.C. Baruah, C.L. Talukdar, *Thermochim. Acta* **218**, 425 (1993)
53. T. Łojewski, K. Zięba, A. Knapik, J. Bagniuik, A. Lubańska, J. Łojewska, *Appl. Phys. A* **100**, 809 (2010)
54. M.-Y. Li, Y. Zhao, T. Tong, X.-H. Hou, B.-S. Fang, S.-Q. Wu, X.-Y. Shen, H. Tong, *Polym. Degrad. Stab.* **98**, 727 (2013)
55. N. Luxford, D. Thickett, P. Wyeth, in *Multidisciplinary Conservation: a Holistic View for Historic Interiors* (Rome, 2010), pp. 1–12
56. A. Deshmukh, S. Deshmukh, V. Zade, V. Thakare, *Int. J. Theor. Appl. Sci.* **5**, 50 (2013)
57. O. Abdel-Kareem, *E-Preservation Sci.* **7**, 40 (2010)
58. J. Szostak-Kotowa, *Int. Biodeterior. Biodegrad.* **53**, 165 (2004)
59. K. Kavkler, N. Gunde-Cimerman, P. Zalar, A. Demšar, *Int. Biodeterior. Biodegrad.* **97**, 51 (2015)
60. J. Nilsson, F. Vilaplana, S. Karlsson, J. Bjurman, T. Iversen, *Stud. Conserv.* **55**, 55 (2010)
61. T. Sawoszczuk, A. Barański, M. Łagan, T. Łojewski, K. Zięba, *J. Cult. Herit.* **9**, 401 (2008)
62. J. Wen, T. Arakawa, J.S. Philo, *Anal. Biochem.* **240**, 155 (1996)
63. S. Podzimek, *Light Scattering, Size Exclusion Chromatography and Asymmetric Flow Field Flow Fractionation* (Wiley, Hoboken, 2011)
64. P. Kratochvil, *Light Scattering from Polymer Solutions* (Academic, New York, 1972)
65. E.S. Sashina, A.M. Bocek, N.P. Novoselov, D.A. Kirichenko, *Russ. J. Appl. Chem.* **79**, 869 (2006)
66. K. Trabbic, P. Yager, *Macromolecules* **31**, 462 (1998)
67. T. Łojewski, P. Miśkowiec, M. Missori, A. Lubańska, J. Łojewska, *Carbohydr. Polym.* **82**, 370 (2010)
68. J. Łojewska, A. Lubańska, P. Miśkowiec, T. Łojewski, L.M. Proniewicz, *Appl. Phys. A* **83**, 597 (2006)
69. P. Calvini, *Cellulose* **19**, 313 (2012)
70. P. Calvini, A. Gorassini, A.L. Merlani, *Cellulose* **15**, 193 (2008)
71. R.J. Heywood, G.C. Stevens, C. Ferguson, A.M. Emsley, *Thermochim. Acta* **332**, 189 (1999)
72. M. Marx-Figini, *Die Makromol. Chem.* **187**, 679 (1986)

73. S. Zervos, A. Moropoulou, *Cellulose* **12**, 485 (2005)
74. M. Strlič, J. Kolar, S. Scholten, in *Ageing Stabilisation Paper*, ed. by M. Strlič, J. Kolar (National and University Library, Ljubljana, 2005), pp. 3–8
75. M. Coppola, M. Djabourov, M. Ferrand, *Macromol. Symp.* **273**, 56 (2008)
76. M.C. Lai, M.J. Hageman, R.L. Schowen, R.T. Borchardt, E.M. Topp, *J. Pharm. Sci.* **88**, 1073 (1999)
77. Y.I. Matveev, V.Y. Grinberg, V.B. Tolstoguzov, *Food Hydrocoll.* **14**, 425 (2000)
78. Y.I. Matveev, V.Y. Grinberg, I.V. Sochava, V.B. Tolstoguzov, *Food Hydrocoll.* **11**, 125 (1997)
79. H. Batzer, U.T. Kreibich, *Polym. Bull.* **5**, 585 (1981)
80. T. Hashimoto, Y. Taniguchi, T. Kameda, Y. Tamada, H. Kurosu, *Polym. Degrad. Stab.* **112**, 20 (2015)